Wind Tunnel Studies on Sawtooth and Monosloped Roofs

David O. Prevatt, P.E., M.ASCE[1]; and Bo Cui, M.ASCE[2]

Abstract: Wind tunnel studies were conducted on 1:100 scale building models of monosloped and several (two- through five-span) sawtooth roof buildings to determine appropriate peak and area-averaged wind pressure coefficients. The results showed that the peak negative pressure coefficients in the high corner regions of monosloped roof buildings are nearly equal to the high corner peak negative pressure coefficients on the windward span (Span A) of the sawtooth roof building, and as expected, low corner zone peak negative pressure coefficients on sawtooth roofs are greater (approximately 150%) than on monosloped roofs. The peak negative coefficients were in general agreement with the earlier wind tunnel study used to develop American wind load design standards, and they suggested that the Australian wind design standard may underestimate the peak loads for moderately sloped (around 20°) sawtooth roofs. Preliminary analyses of the data suggest that current ASCE 7 wind design provisions for monosloped roof buildings may underestimate the high corner design wind pressure. However, this may be offset by a more rapid decrease in area-averaged peak pressure coefficients with increasing tributary areas than was previously observed in the earlier studies.

DOI: 10.1061/(ASCE)ST.1943-541X.0000200

CE Database subject headings: Wind tunnels; Buildings, low-rise; Building envelope; Roofs; Failures; Uplifting; Wind loads; Wind pressure.

Author keywords: Wind tunnel testing; Buildings, low-rise; Envelope; Roofs; Roof failure; Uplift resistance; Wind loads; Wind pressure.

Introduction

Current wind design provisions are based on wind tunnel testing conducted from the late 1970s through 1990s on several building shapes. However, wind tunnel studies were conducted on sawtooth roof buildings (Holmes 1983, 1984, 1987; Saathoff and Stathopoulos 1992), and they provide the database used to develop the Australian (Standards Australia 2002) and American (ASCE/SEI 2006) wind load provisions. The conclusions regarding the peak wind uplift loads on sawtooth roofs in those papers do not agree and those discrepancies are yet to be resolved. As a result, significant discrepancies remain between the U.S. and Australian wind load design provisions calculated for identical buildings in accordance with ASCE 7-05 and AS/NSZ 1170 (see Table 1).

The high corner peak design pressures for components and cladding based on ASCE 7 (ASCE/SEI 2006) are approximately 74% greater than AS/NSZ 1170 (Standards Australia 2002) design wind pressures. Given different philosophies and design approaches among international codes, it is not expected that design values should be identical. However, such a large discrepancy suggests a need for further studies.

The objective of this study is to determine and compare the peak local and peak area-averaged wind pressure coefficients on monosloped and sawtooth roofs in an effort to resolve existing discrepancies between previous wind tunnel studies and existing building codes. This study uses larger scale models (1:100 scale) than were used previously and a dense 290 pressure tap array providing a single pressure tap tributary area of less than 0.42 m^2 or 0.2% of total roof monitor area.

Sawtooth Roofed Building

Sawtooth roof buildings consist of a series of single-pitch roof monitors (or raised roof sections), arranged in a serrated edge profile, akin to the teeth of a saw blade (Fig. 1). The sawtooth building finds use in factories, gymnasia, and buildings that require large open spaces. An important feature is the vertical wall of each roof monitor which provides locations for large window openings to allow natural daylight to enter the buildings.

In the classic sawtooth roof building, the low edge of one monitor roof meets or is located near to the bottom edge of the vertical monitor wall of the adjacent roof monitor. A variation of the classic sawtooth roof structure is the "separated-sawtooth" roof, which also has several sloped roof monitors placed some distance apart. This distance can vary from 1 or 2 m to exceeding the width of the monitor roofs themselves. Current wind design codes are silent on design methods applicable to separated-sawtooth buildings and whether there should be a "threshold" separation distance beyond which design criteria for the monosloped roof should prevail.

[1]Assistant Professor, Dept. of Civil and Coastal Engineering, Univ. of Florida, 365 Weil Hall, P.O. Box 116580, Gainesville, FL 32611-6580 (corresponding author). E-mail: dprev@ce.ufl.edu

[2]Structural Engineer, Rig Package Engineering Group, 10000 Richmond Ave., Houston, TX 77042; formerly, Graduate Student, Clemson Univ., Clemson, SC 29634. E-mail: bo.cui@nov.com

Note. This manuscript was submitted on May 4, 2009; approved on February 3, 2010; published online on February 8, 2010. Discussion period open until February 1, 2011; separate discussions must be submitted for individual papers. This paper is part of the ***Journal of Structural Engineering***, Vol. 136, No. 9, September 1, 2010. ©ASCE, ISSN 0733-9445/2010/9-1161–1171/$25.00.

Table 1. Peak Negative Components and Cladding Design Pressures (in kN/m^2) on Identical Buildings Using ASCE 7-05 (ASCE 2005) and AS/NSZ 1170 (Standards Australia 2002) Provisions for 16-m-Tall Rectangular Enclosed Buildings with One Wall Permeable, Other Walls Impermeable, 21° Roof Slopes, and Height to Width Ratios as Shown; Basic (Noncyclonic) Design Wind Velocity Is 58 m/s in Open Exposure and the Effective Tributary Areas Are 1 m^2 or Less

	Height to width ratio	ASCE 7-05[a] (kN/m^2)	AS/NZ 1170[b] (kN/m^2)	(ASCE 7/AS/NSZ) (%)
Single-span buildings				
Monosloped	1.52	−6.3	−4.3	146
Gable roof	1.52	−5.8	−4.3	133
Multispan buildings				
Multigable	0.38	−6.0	−3.3	178
Sawtooth windward span	0.38	−8.5	−4.9	174
Sawtooth leeward span	0.38	−5.8	−2.9	200

[a]ASCE 2005.

[b]Standards Australia 2002.

In this paper, results are discussed in terms of six roof pressure zones and up to five roof monitor (or span) locations. Each roof monitor has a high edge, a low edge, and two sloping edge zones, located along the respective boundaries as shown in Fig. 2. The "high corner" zone is located at the high edge/sloping edge intersections and the "low corner" zone is located at the low edge/sloping edge intersection. The interior zone is located within the boundaries of the five zones previously defined.

Previous Studies

Monosloped Roof Wind Tunnel Studies

Stathopoulos and Mohammadian (1985) conducted an extensive study at the Concordia University wind tunnel using a 1:200 scale monosloped model with a 4.8° roof slope to evaluate the effects of building widths and height on pressure coefficients. The largest local peak negative pressure coefficients observed were −6.3 (normalized to hourly wind speed at mean roof height), occurred at the high corner of the roof, and −4.77 at the low corner. The study also concluded that higher pressure coefficients occur on larger scale models by comparing the mean and peak pressure coefficients from a 1:200 scale model with those from a 1:400 one. The writers concede that the pressure tap locations on the two models were not identical and some data were missing from the larger model.

Another interesting finding was made by comparing pneumatically and arithmetically averaged area pressure coefficients. The roof (with full-scale dimensions of 61 m × 24.4 m) was divided into 20 panels of approximately equal size (74 m^2 having three to four taps per panel). The study found close similarity between pneumatically and arithmetically averaged mean pressure coefficients and peak negative pressure coefficients. However, for extreme pressure values of −1.75 or more, pneumatically averaged pressure coefficients were slightly less negative than the magnitudes of numerically averaged ones. Data obtained by Stathopoulos and Mohammadian (1985) using the University of Western Ontario monosloped roof model with a variable roof slope, of 1:12, 2:12, and 4:12, showed that the mean pressure coefficients appear to decrease at the lower eave and increase at the ridge with increasing roof slope. Peak pressure coefficients also increased at the ridge with increasing roof slope but were unaffected at the lower eave.

Fig. 1. Classic four-span sawtooth roof building with windows installed in vertical wall of roof monitors

Fig. 2. Naming convention for the six roof zones

Sawtooth Roof Wind Tunnel Studies at CSIRO, Australia

Holmes (1987) reported research findings from a two-part study of wind loads on sawtooth roof buildings conducted at the Commonwealth Scientific and Industrial Research Organization (CSIRO) boundary layer wind tunnel These reports present results for point pressures (Part I) (Holmes 1983), and panel pressures (Part II) (Holmes 1984). Wind tunnel studies were conducted on a 1:200 scale five-span sawtooth roof model structure, having a 20° roof slope. The full-scale dimension of each roof monitor was 12 m by 38.8 m and the mean roof height was 11.8 m. Seventy-two pressure taps were installed on the sloping roof, 10 taps on vertical faces, and 40 pressure taps on the walls. Mean and peak pressures were monitored for five wind directions (0°, 45°, 90°, 135°, and 180°). The highest individual peak suction was a value of −7.3, occurring in the high corner zone of Span A (windward span) (normalized to 10-min mean wind speed at low eave height).

Table 2. Local Peak Pressure Coefficients on Sawtooth and Monosloped Roof Buildings (Saathoff and Stathopoulos 1992)

	Monosloped roof	Sawtooth roofs					
	One span[a]	Two spans[a]		Four spans[a]			
Roof pressure zone	*A*	*A*	*B*	*A*	*B*	*C*	*D*
High corner	−9.8	−10.2	−6.4	−10.2	−5.6	−5.5	−4.8
Low corner	−4.7	−6.3	−5.3	−7.9	−7.7	−7.3	−6.0
Interior	−3.3	−3.8	−3.2	−4.1	—	—	−3.2
High edge	−4.2	−6.2	−5.8	−5.5	−4.5	−3.8	−3.6
Low edge	−3.2	−3.2	−3.2	−3.7	—	—	−2.9
Sloped edge	−3.8	−5.1	−4.9	−5.8	−5.4	−4.7	−4.3

[a]Saathoff and Stathopoulos 1992; referenced to mean-hourly wind speed at low eave height of building. Spans are identified alphabetically from windward to leeward side of building.

In Part II pneumatically averaged pressure measurements taken on the roof were determined using 10 pressure taps manifolded together to represent a roof panel measuring 34 m^2 at full scale. The most extreme mean pressure coefficient observed was −1.7 and the most extreme peak negative pressure coefficient was −3.86, both occurring on a high corner panel for the 45° wind direction.

While Holmes suggested that both pneumatic and arithmetic averaging methods may slightly overestimate peak panel loads, he argued that using higher density of closely spaced pressure taps should reduce this error. It should be noted that the arithmetic averaging technique shows significant overestimation when lack of correlation of action of the local point pressures is neglected (Stathopoulos 1982). As such, both high tap density and pressure correlation are incorporated in the adopted methodology described later in this paper.

Sawtooth Roof Wind Tunnel Studies at Concordia University, Canada

Saathoff and Stathopoulos (1992) used 1:400 scale models with 72 roof pressure taps to determine local and area-averaged wind pressures on a monosloped roof and on two- and four-span sawtooth roof models. Stathopoulos and Saathoff (1992) reported that the maximum negative pressure coefficient of −10.0 (normalized to mean dynamic pressure at lower eave height) occurred in the high corner region of the monosloped roof and Span A of the sawtooth models. Peak values of negative pressure coefficient in the low corners ranged from −7.9 on Span A to −6.0 on Span D and −4.7 on the monosloped roof low corner. There are three pertinent findings from this study which will be discussed in detail as follows:

1. The peak local pressure coefficients in the high corner roof zones in this study were larger than that obtained by Holmes (−10.0 versus −8.2). Note that, for comparison purposes, the Holmes peak coefficients were scaled up 12% by the square of velocity ratio (-7.3×1.12) to account for the shorter averaging time used (see Tables 2 and 3).
2. The peak and mean pressure coefficients on the monosloped roof closely match the corresponding values on Span A (windward span) sawtooth roof model having similar roof monitor geometry. The peak pressure coefficients were over 50% larger than the earlier results by Stathopoulos and Mohammadian (1985) for monosloped roof structures.
3. The area-averaged peak negative pressure coefficients remained almost constant for a tributary area range of 0.1–10 m^2 (using two pressure tappings) and decreased for tributary areas over 36 m^2 (using four pressure tappings).

Wind design pressure coefficients on sawtooth roofs were included in the 1995 edition of ASCE 7. Despite the geometric similarity between a sawtooth roof monitor and monosloped roof structures and corroborating experimental results presented by Saathoff and Stathopoulos (1992), the peak design pressure coefficient for the high corner region of the monosloped roof is still 30% lower than that for the high corner of the windward span (Span A) sawtooth roof.

Table 3. Local Peak Pressure Coefficients on Five-Span Sawtooth Roof Buildings (Holmes 1983)

	Sawtooth roof				
	Five spans[a]				
Roof pressure zone	*A*	*B*	*C*	*D*	*E*
High corner	−5.4 (−7.3)	−3.9	−4.0	−3.8	−3.9
Low corner	−3.8	−3.9 (−5.9)	−4.0 (−5.9)	−3.8	−3.9
Interior	−2.6	−2.9	−2.8	−2.8	−2.9
High edge	−2.7	−2.3	−2.1	−1.8	−2.5
Low edge	−2.1	−1.4	−0.9	−0.9	−1.7
Sloped edge	−3.8 (−3.3)	−3.9	−3.9	−3.8	−3.9

Note: Values in parentheses represent estimates of individual peak pressure value made from several runs. Other values represent average value of peak pressures for all individual points within each zone.

[a]Holmes 1983; referenced to 15-min mean wind speed at low eave height of building. Spans are identified alphabetically from windward to leeward side of building.

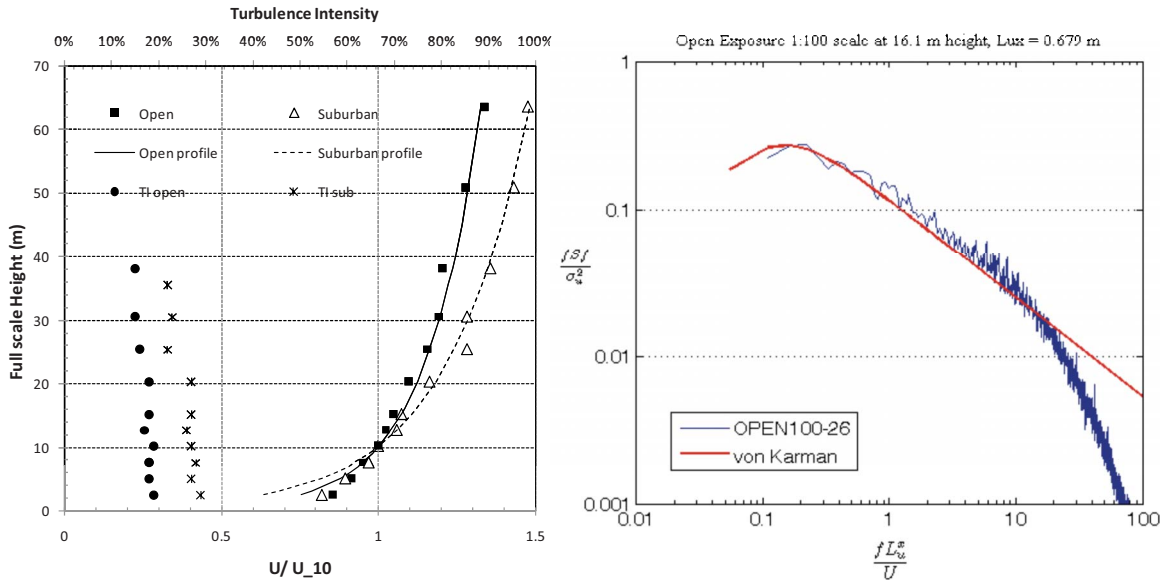

Fig. 3. (a) Velocity and turbulence intensity profiles for open country and suburban exposures and (b) normalized power spectra for open exposure at 16.1 m

Experimental Setup

The wind tunnel configuration, scale model construction, instrumentation, and test procedures are described in the following sections. A full description of the experimental procedure, results, and additional analyses is contained in Cui (2007).

Boundary Layer Wind Tunnel

Wind tunnel studies were conducted in Clemson University's boundary layer wind tunnel, which is an open-return wind tunnel with an 18 m (48 ft) long by 3 m (10 ft) wide by 2.1 m (7 ft) tall test section that is powered by two 1.8-m (5-ft) diameter fans. Wind flows through a settling chamber, contraction cone, and several screens and honeycombs before entering the test section with near uniform wind speed and minimal turbulence across the test section entrance. Test models are mounted on the 2.7-m (9-ft) diameter turntable, approximately 15 m from the test section entrance. The turntable allows full 360° rotation to test model for any desired wind azimuth.

Trip plates and spires are set up at the entrance to the test section, which, in addition to the slant boards and roughness elements, arranged along the test section to initiate the growth of a thick simulated atmospheric boundary layer at model scale. We simulated the upwind terrain at 1:100 geometric scale and modeled the velocity profile and turbulence intensity for open country and suburban exposures. The wind speed at reference height in the tunnel (300 mm below tunnel ceiling) was approximately 13 m/s for both exposure conditions.

Velocity Profiles

Wind flow characteristics in the wind tunnel are measured using hot-wire probes and a Thermal System Incorporated IFA300 constant temperature hot-film anemometer system. Wind speed data are taken at 4,000 samples/s for 65 s at each height above ground in the location of the model (with the model removed), and the mean wind speed and turbulence intensities are determined. The wind tunnel measurements were a good match for logarithmic velocity profile up to about 60 and 80 m in open country and suburban terrain exposures, respectively. The roughness lengths z_0 for open country and suburban terrain exposures were 0.034 and 0.22 m, respectively. Mean velocity and turbulence intensity profiles are shown in Fig. 3(a). Eq. (1) provides the logarithmic law profile for comparing velocities. The mean wind speed at reference height (300 mm below the top of the tunnel) was 13 m/s. Power spectra and turbulence length scale for open country exposure are provided in Fig. 3(b)

$$\frac{U_z}{U_{10\ \mathrm{m}}} = \left[\frac{\ln(z/z_0)}{\ln(10/z_0)}\right] \tag{1}$$

The longitudinal integral length scale of turbulence at roof height (16.1 m) of the wind flow was 0.678 m (68 m at full scale). While this value may appear low, it is a reasonable compromise for wind tunnel studies of cladding pressures on a large-scale low-rise building. Also, it is within the order of magnitude of other published data (Garg et al. 1997; Richards et al. 2007; Tieleman et al. 1981). Since the longitudinal integral length scale is larger than the largest model size, large-scale eddies will fully engulf the model building and from that point on, the increase in longitudinal integral length scale is not an important factor in the load simulation (Tieleman 1982). Further, Holmes (1982) suggested that ratios of desired turbulence scales down to 0.5, which are tolerated for low-rise building measurements where local cladding pressures only are of concern, particularly for the 1/100 and 1/50 scale experiments.

Scale Model and Pressure Measurement System

Pressure taps were installed on the roof of one span of the sawtooth building model. The wind tunnel pressure data were collected using eight Scanivalve ZOC33 electronic pressure scanning modules connected to a RAD3200 digital remote analog to digital converter. This system allows near-simultaneous sampling of maximum of up to 512 pressure taps. Tap pressure data were sampled at 300 Hz. The mean wind speed at mean roof height of

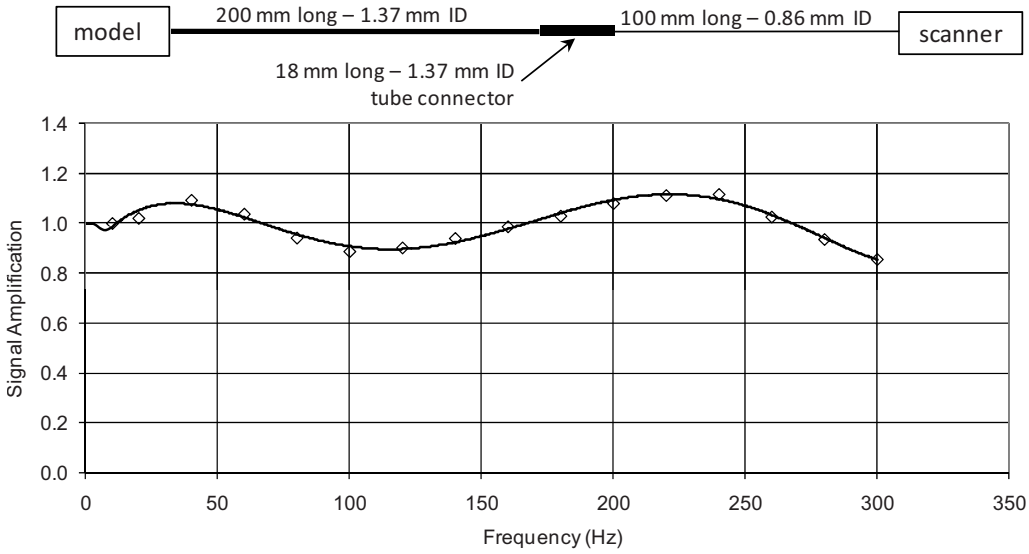

Fig. 4. Frequency response and arrangement of the pressure tubing system

the model was 6.0 m/s, and the reference wind speed (measured by a reference Pitot tube 300 mm below the top of the tunnel) was 13 m/s.

Tubing System

A 300-mm (12-in.) long tubing system was used to connect each pressure tap to the pressure scanning modules. The tubing system consists of a 200-mm-long, 1.37-mm (0.054-in.) internal diameter (ID) vinyl tube connected to the model, a 100-mm-long, 0.86-mm (0.034-in.) ID vinyl tube connected to the pressure scanner, and an 18-mm-long, 1.37-mm (0.054-in.) ID brass tube connecting the two vinyl tubes (top of Fig. 4).

The dynamic amplification correction methodology used here is based on the approach detailed by Irwin et al. (1979). The tubing system's frequency response was determined by comparing the direct (no tubing) measurement of a white noise signal with the measurement after passing through the tubing system. The tubing response was determined up to 300 Hz as shown in Fig. 4 along with a sketch of the tubing system arrangement. The worst case dynamic amplification was less than $\pm 10\%$. Irwin et al. (1979) found that the phase distortion on measured peak pressures was small for short tubes [0.6 m (24 in.) or less]. For this experiment, which uses 300-mm tubing lengths, the phase distortion correction was neglected. The dynamic amplification for each tap was removed by adjusting the signal in the frequency domain before analyzing the wind tunnel data.

A reference Pitot tube installed 300 mm below the top of the wind tunnel test section (180 m at full scale) provided the reference static pressure for normalizing the surface pressures on the model and a measure of the mean wind velocity in the tunnel. The pressure coefficient was determined as follows:

$$C_p = \frac{p_i}{\frac{1}{2}\rho V^2_{ref,z_0,meanhrly}} \tag{2}$$

where pressure coefficient C_p=ratio of pressure at each tap p_i divided by the dynamic pressure due to mean wind velocity at reference height in the wind tunnel, $V^2_{ref,z_0,meanhrly}$. ρ is the air density.

Model Construction

The geometry of the 1:100 scale building model was selected to match an existing sawtooth building inspected by the first writer. In addition, this roof slope closely matches the roof slope (20°) of the model tested by Saathoff and Stathopoulos (1992), which provides the experimental results for wind pressure coefficients in ASCE 7-05 (Figs. 6–15):Sawtooth Roofs, page 63 of ASCE 7-05, "Minimum design load for buildings and other structures" (ASCE/SEI 2006).

The sawtooth building models were constructed by combining several monosloped roof models, each having a 21° roof slope. In this way, tests were conducted on a monosloped roof and on two-, three-, four-, and five-span sawtooth roof building models. The tests also included three building heights corresponding to full-scale mean roof heights of 7, 11.6, and 16.1 m. The sawtooth roof spans were designated in conformance with ASCE 7 naming conventions. For instance, for a five-span sawtooth structure the windward span is called Span A, the "middle" or interior spans designated alphabetically by Spans B, C, and D, and the leeward span by "Span E."

The five single pitched models were constructed using Plexiglas sheet and 290 pressure taps were installed in one of the model roofs. Ten pressure taps were installed vertically along the centerline of the two roof monitor side walls. Due to symmetry, the pressure tappings on only approximately one-half of the roof monitor have been used. Additional pressure taps were installed in the vertical wall of the roof monitor and the side walls to assess scaling of pressure coefficients. The monosloped building model is 79 mm wide by 299 mm long, with adjustable inserts to form three building heights with mean roof heights of 70, 116, and 161 mm. The location of the instrumented span was changed during the tests in order to collect wind pressure data for the whole sawtooth roof system. Fig. 5 shows these assembled sawtooth roof models with the respective model geometry information. Since the model occupies less than 1% of the tunnel cross section, blockage effects are not a factor [ASCE (1987)].

Table 4 compares pertinent experimental details from this study with the two previous studies. It should be noted in addition to using a larger model scale the number of taps has been increased resulting in a dense pressure tap area that has a minimum

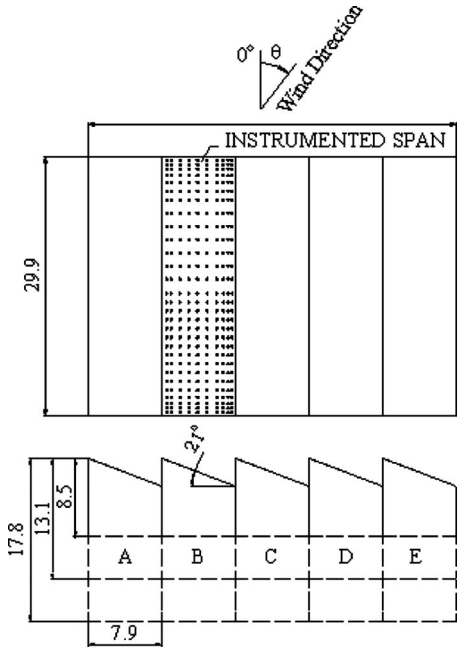

Fig. 5. Plan and elevations of sawtooth building models (dimensions are in meters)

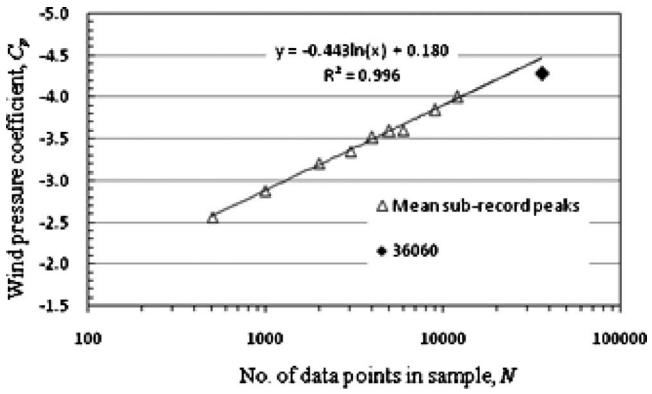

Fig. 6. Peak suction coefficients for subrecords in sample compared with measured peak value

pressure tap tributary area of just 0.42 m^2 and distance from nearest pressure tap to the high edge of only 0.38 m at full scale.

The results in this paper are limited to comparing pressure coefficients for a monosloped roof structure with a mean roof height of 16.1 m tall with values on two- through five-span sawtooth roofs. The effect of building height, separation distances, and terrain exposures on roof pressures are included in Cui (2007) and will be addressed in a forthcoming paper.

Experimental Procedure

Based on the one to four velocity scale (13 m/s in wind tunnel versus 58-m/s design wind velocity), sampling frequency, and the 1:100 geometric length scale, the 120-s sample time corresponds to a full-scale record of approximately 50 min, which is sufficient to provide a stable estimation of the peak wind pressure. An extrapolation method was used for determining peak pressure coefficients from the single wind tunnel runs. Each 120-s wind tunnel record (sample frequency of 300 Hz) consisted of 36,060 readings and it was divided into several equal-length subrecords and the average of the statistical value (mean, minima or maxima, etc.) calculated for each subrecord. By varying the subrecord length into nine sets, ranging from 500 up to 12,000 samples, and repeating this process, a series of values was obtained and used to predict the statistic for the whole record by linearly regressing the data on a semilogarithmic plot.

For all wind directions except critical cornering winds no repeats were considered necessary. However, a check was made at the critical wind (cornering) directions by evaluating pressure coefficients for 8 or 16 repeats. The results of the extrapolation were consistent with these results. The regression equation was then used to predict the expected peak for each full-length record, as illustrated in Fig. 6.

For the illustrated case, the extrapolated peak negative pressure coefficient was −4.47, which compares favorably with the actual measured peak pressure coefficient of −4.29 for this full record. In addition, the peak estimate extrapolation method was validated by comparing its results with peak pressure coefficient estimates obtained using the Lieblein BLUE method to fit points to the Type I extreme distribution (Lieblein 1974) and by a direct peak averaging techniques from multiple (8 and 16) runs for each wind direction. The extrapolated peak estimates were found to have excellent agreement with results from the latter two approaches.

In the results that follow, the sawtooth spans were named Span A (windward span) through Span E (the leeward span of the five-span sawtooth model). All internal spans (i.e., Spans B, C, and D

Table 4. Comparison of Wind Tunnel Test Setup between Current Study and Prior Sawtooth Roof Wind Tunnel Tests

	This study	Saathoff and Stathopoulos (1992)	Holmes (1983)
Model scale	1:100	1:400	1:200
Models tested	Mono, two-, three-, four-, and five-span sawtooths	Mono, two-, and four-span sawtooths	Five-span sawtooth
Prototype dimensions	7.9 m × 29.9 m × 16.1 m	19.4 m × 61 m × 14.6 m	12 m × 39 m × 11.8 m
($B \times W \times$ mean roof height)	× 11.6 m	—	—
	× 7.0 m	—	—
Roof slope	21°	15°	20°
Wind directions tested	0°–350° at 10° intervals	0°, 30°–150° at 15° intervals, 180°	20°–60° at 5° intervals
Number of pressure taps (roof)	290	72	60
Minimum tap tributary area	0.42 m^2	5 m^2	3.2 m^2
Distance to nearest edge	0.38 m	0.6 m	2.0 m
Sample time/sample frequency	120 s/300 Hz	16 s/500 Hz	11.5 s/3000 Hz

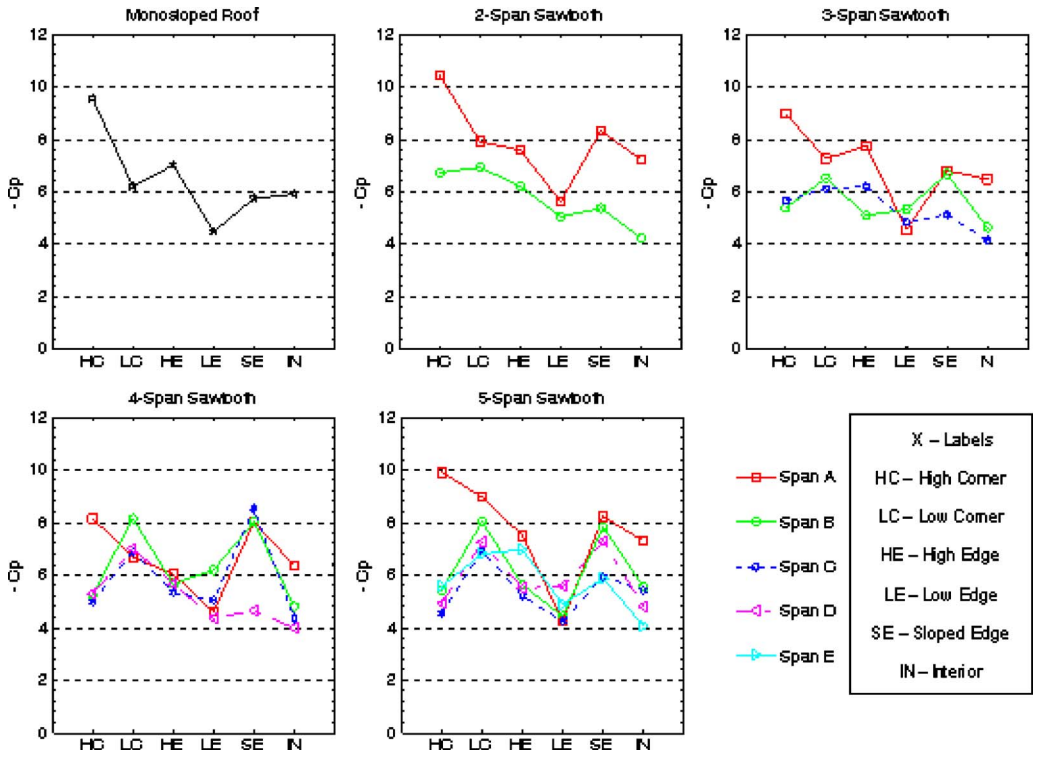

Fig. 7. Peak negative pressure coefficients on the six roof zones for monosloped and two- through five-span sawtooth roof buildings. Pressure coefficients are normalized to the mean-hourly wind speed at mean roof height (16.1 m) of the buildings.

on the five-span building, B and C on the four-span model, and Span B on the three-span models) were designated as middle spans and treated together. The "leeward" spans were Span E of the five-span, Span D of the four-span, Span C of the three-span, and Span B of the two-span building models. The dimensions for the six roof zones were established using ASCE 7 provisions and the same dimensions were used with all building walls. The edge zones were 1.8 m wide, resulting in a low corner zone having a square plan 1.8 m on side. The high corner zone was 3.6 m long for the windward span and 1.8 m for all other spans.

Results

Local Peak Pressure Coefficients

Fig. 7 presents the negative pressure coefficient relationships for the six roof zones and five building shapes tested. It is observed in all cases that the highest negative pressure coefficient was observed in the high corner of the windward spans, and these values ranged from −10.41 on the two-span roof, −9.89 on the five-span roof, −8.94 on the three-span roof, and −8.15 on the windward span of the four-span sawtooth roof building. The comparable high corner peak pressure coefficient for the monosloped roof building was −9.54, similar to previous findings by Saathoff and Stathopoulos (1992).

Pressure coefficients measured in the high corner zones are significantly reduced for the middle and leeward spans of all sawtooth buildings. The low edge and interior regions of all roofs experienced the smallest peak pressure coefficients in all cases tested. The highest peak pressure coefficients observed on the leeward and middle spans occurred at the low corners (−8.13) and sloping edge regions (−8.54). These results also generally agree with previous findings.

Wall pressures were also monitored at the 10 pressure taps installed vertically along the centerline of the roof monitor side walls. Highest negative pressure coefficients observed ranged from −4.0 to −3.73, observed at the monosloped model and the leeward span of the sawtooth roof, for incident winds approaching perpendicularly to the high edge.

Contour plots of peak negative wind pressure coefficients for all wind directions are illustrated in Fig. 8 for approximately half of the roof surface. It can be seen that the magnitudes and pressure distribution on the sawtooth building models are similar to that on the monosloped roof except that additional peak pressures occur near the low corner zones of the sawtooth buildings. The high corner peak values are observed to extend well beyond the ASCE 7 defined high corner region for the monosloped roof.

Fig. 9 presents the peak negative pressure coefficients for various roof zones on all building models tested. The data were found to collapse very well throughout the various roof spans, consistently indicating the highest pressures in the high corner regions of the windward spans (Span A). At the high corner and high edge zones, the data suggest an aspect ratio effect where the middle spans experience lower peak pressures than either the windward or leeward spans. Generally, except for the low corner, the peak pressures on the monosloped roof structures were observed to be consistent with pressures on the sawtooth roof structures.

Area-Averaged Pressure Coefficients

The wind load design of components and cladding utilize both the local peak pressure coefficients (i.e., for individual mechanical fasteners with small tributary areas) and the area-averaged wind pressure coefficients for establishing wind design loads on larger tributary area roof systems (i.e., single-ply membranes). In contrast to the local peak pressure coefficients presented in the previous section, area-averaged pressure coefficients are determined

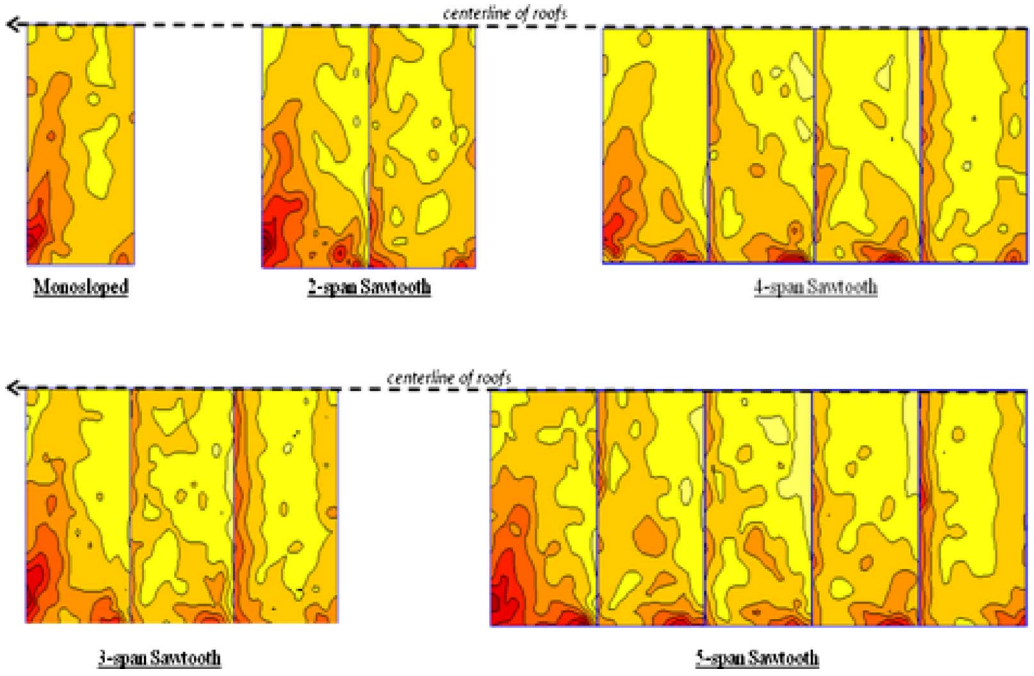

Fig. 8. Contour plots showing the peak negative pressure coefficients for the 16.1-m set of buildings, normalized to mean-hourly wind speeds at mean roof height

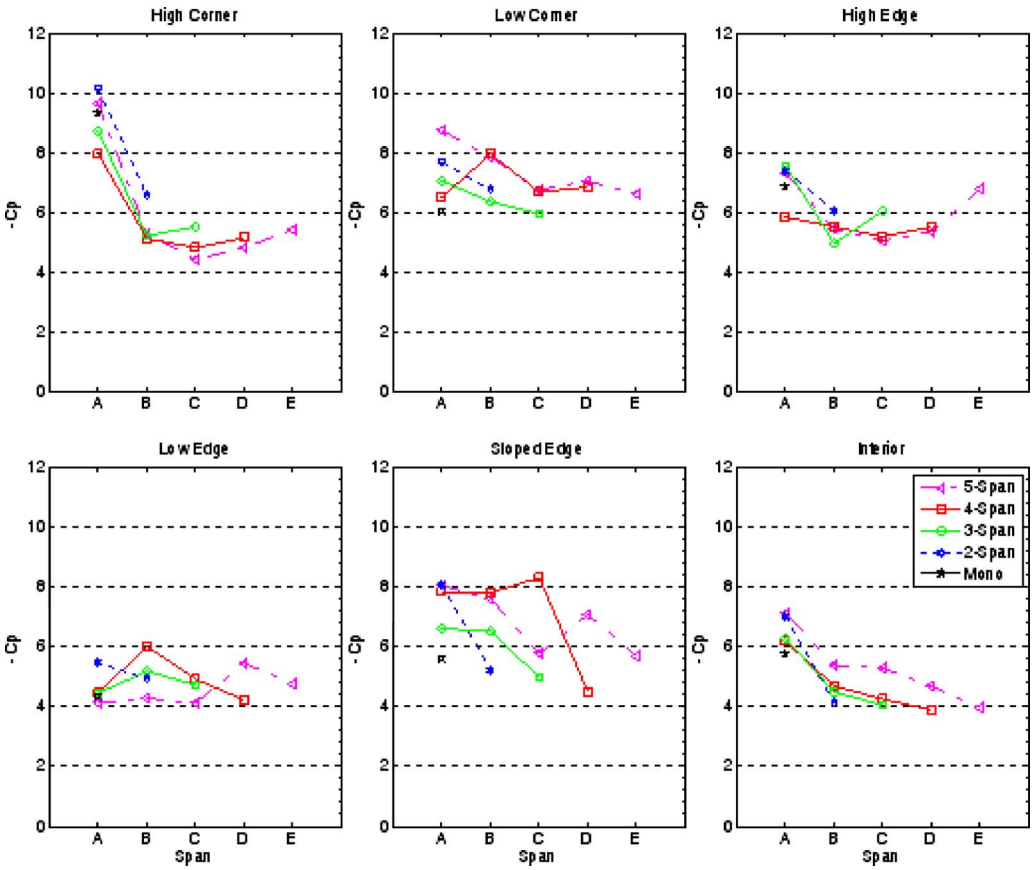

Fig. 9. Comparing the peak negative pressure coefficients for the five building models tested (normalized to mean wind velocity at mean roof height)

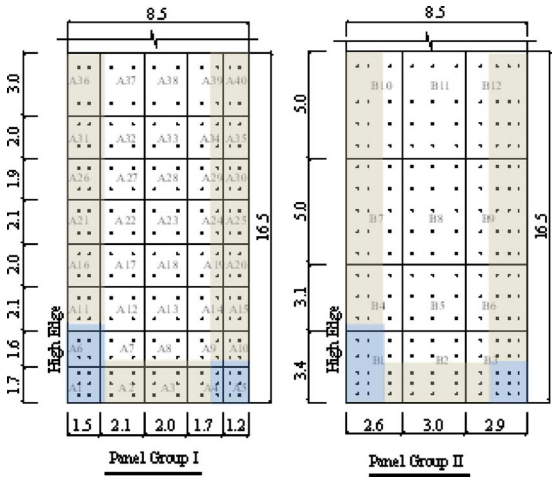

Fig. 10. Location of area-averaged tributary panel areas in Panel Groups I and II in relation to the roof corner and edge regions (approximate dimensions are in meters)

using data from several pressure taps within a region, and they provide the average pressure acting on the region represented by the tributary areas of the taps.

The previous studies had used pneumatic integration methods (several pressure taps physically connected through a pressure manifold to a single pressure tube) to estimate area-averaged pressure coefficients. In this study, a numerical integration approach was used enabling greater combinations of pressure taps to be studied from a single set of wind tunnel data. Numerical averaging was carried out using the pressure coefficient time histories for pressure taps, factored by their respective tap tributary areas. The time series of area-averaged wind pressure coefficients were determined by integrating the local wind pressure coefficient time series for pressure taps within the specified areas using the following equation:

$$C_{p(area,j)} = \frac{\sum_{i=1}^{n} (C_{p(i,j)} A_i)}{\sum_{i=1}^{n} A_i} \tag{3}$$

where $C_{p(area,j)}$=area-averaged wind pressure coefficient at time step j; $C_{p(i,j)}$=instantaneous local wind pressure coefficient of pressure tap i at time step j; n=number of pressure taps in the specified area; and A_i=tributary area of the ith pressure tap.

Once the area-averaged pressure time series is created, the pressure coefficient statistics representative for the area are developed by extrapolation as described for the single pressure tap. Numerical integration of pressures offers considerable flexibility for selecting the tributary area shapes and sizes, and potential errors are minimized by using high tap density and small tributary areas. Further, this technique incorporates the correlated action of the independent peaks, suggested by (Stathopoulos 1982), by constructing a representative pressure time-history from individual measurements.

Area-averaged wind pressure coefficients were determined for tributary areas within the high corner and low corner regions, ranging from 0.9 m^2 (for two pressure taps) to 37.1 m^2 (for 49 pressure taps). In addition, area-averaged values were obtained for two panel groups, shown in Fig. 10, where tributary areas of panels ranged from 1.8 to 5.8 m^2 in Panel Group 1 and from 7.4 to 15.8 m^2 in Panel Group 2.

Fig. 11 presents a comparison of the peak area-averaged negative wind pressure coefficients for the 16.1-m-high monosloped roof and the windward spans of 16.1-m-high two- to five-span sawtooth roofs. These results are also compared with previous data from Saathoff and Stathopoulos (1992). The area-averaged pressure coefficients are significantly reduced from the peak local pressure coefficients in all roof regions. The larger the tributary area, the greater is the reduction observed. For the Panel Group I, up to 2.5 m^2 (equivalent to individual fastener tributary areas), a 32–39% reduction was observed in the high corner regions on the windward span and nearly 50–60% reduction on the larger Panel Group II areas (8–9 m^2) (equivalent to single girt or secondary member tributary area).

Discussion

The results presented in this paper have shown the benefits of using larger scale wind tunnel models with denser pressure tap arrangements. The results are directly comparable to previous results as the pressure coefficients are normalized to the mean wind velocity at mean roof height. The adjustment needed because previous data were normalized to lower eave height is not expected to be significant, given the small height difference involved. It is observed that peak negative pressure coefficients in the high corner regions of the windward spans are nearly equal to previous data and that the trends in the data for all roof zones are also similar. The results appear to be consistent with previous findings by Saathoff and Stathopoulos (1992) and that peak pressure coefficients obtained by Holmes (1987) may underestimate the high corner wind pressures on sawtooth roofs. The reader is cautioned in the difficulty of direct comparison of pressure coefficients from different experiments using models with different roof slopes. However, that Holmes results obtained a lower value may be explained because the pressure tappings were located relatively far away (2 m at full scale) from the roof boundaries and would be less likely to experience the vortex-induced peak suctions. Further, Stathopoulos and Mohammadian (1985) suggested peak pressures along the ridge increases with increasing roof slope, which may also contribute to the higher peak pressures in the 20° sawtooth roof model. While the results suggest that Holmes (1987) somewhat lower peak pressures may not be appropriate for wind design loads for steeper sloped (greater than 5°) sawtooth roofs, further confirmatory analysis is in progress, to be included in a forthcoming paper.

Overall trends in the results are also consistent with previous results reported in the literature, with the highest wind pressure coefficients occurring in all roof zones on the windward spans and reduced wind pressure coefficients on the middle and leeward spans. The results presented here do not indicate any significant differences between the high corner peak wind loads on monosloped roofs and the windward span of sawtooth roofs of two through five spans. In fact, validation is established (in a forthcoming paper); ASCE 7-05 peak pressure coefficients for monosloped roofs may be underestimated.

Using large models with greater tap densities and the flexibility of the numerical averaging techniques the area-averaged pressure coefficients differ somewhat from previous studies. The results revealed a faster falloff of peak pressure coefficients with increasing tributary area on the windward spans and monosloped roof. It was found that the area-averaged pressure coefficients (for

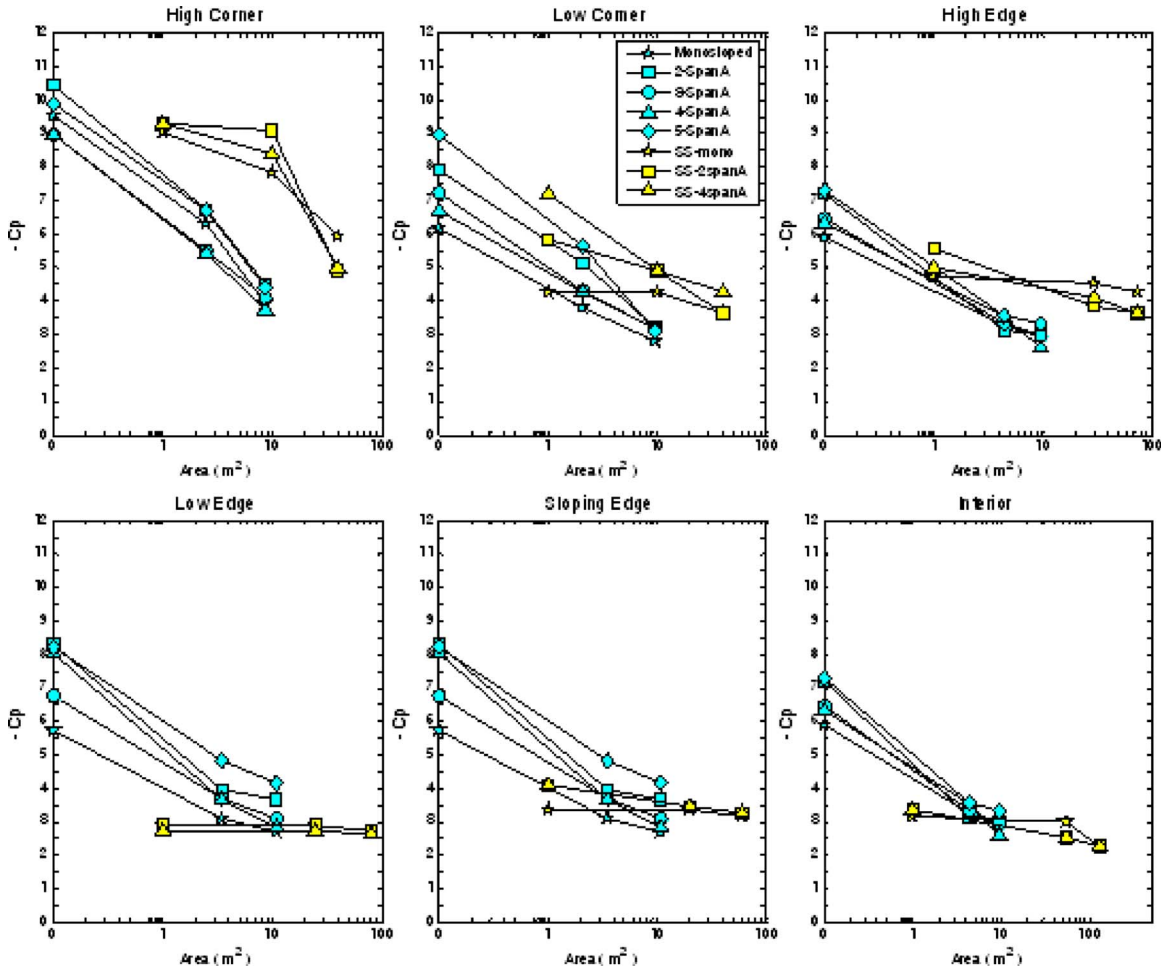

Fig. 11. Variation of area-averaged pressure coefficients with tributary area from present study (tributary areas up to 10 m^2), compared with data adapted from Stathopoulos and Saathoff (1992)

four to six pressure taps) in relatively small tributary areas (2.5 m^2 or less) were reduced by over 50% from the highest local peak pressure coefficient in the high corners and near to 60% reduction in the low corners. As the tributary area is increased to 10 m^2, the area-averaged pressure coefficients on the windward span areas were observed to reduce to 58% (along high edge) to 138% (low corner) less than equivalent local peak pressures. Previous studies had found only small reductions in pressure coefficient up to 10-m^2 tributary areas, but these were determined using only two pressure taps on smaller scale models. These results are likely to have significant impact on the wind code values for sawtooth and monosloped roof systems.

This wind tunnel study has also confirmed that there is no significant difference in extreme negative pressure coefficients on monosloped roofs and the windward spans of sawtooth roofs. The results call into question the current wind design values in ASCE 7 for monosloped roofs, which were probably based on the 1985 study by Stathopoulos and Mohammadian.

The effect of downstream sections of the sawtooth roof and overall building aspect ratios may be a factor in the range of peak pressures observed for the two- through five-span sawtooth models, but no definitive trend was established. In a subsequent paper, detailed results will be presented to compare the effects of building height and separation distance in sawtooth roofs to provide suggestions for modifying the current wind design code provisions for sawtooth and monosloped roof buildings.

Conclusions

This paper described a wind tunnel investigation that was conducted using 1:100 scale models of monosloped and sawtooth roof structures. The models were constructed with a dense pressure tap array and results recorded to determine the peak local and area-averaged pressure coefficients in several roof zones. The motivation for the study was to determine the basis of a discrepancy in wind design values between the Australian and North American wind load design standards for sawtooth roof structures. The results were compared with results from previous experimental studies and to determine the effect of roof span location. The following important conclusions were made:

- The peak negative pressure coefficients measured at the high corner of the monosloped roof are nearly the same as occurs on the high corner of the windward span (Span A) of the sawtooth roof. The results suggest that current ASCE 7 peak design pressure coefficients for monosloped roof structures may be unconservative.
- The peak local pressure coefficient results in this study generally agree with findings by Saathoff and Stathopoulos (1992) and were higher than the peak pressure coefficients obtained by Holmes (1987). Holmes' results may be appropriate for lower slope sawtooth structures but may underestimate the peak local pressures on the windward ("A") spans of steeper

sawtooth roofs. The higher peak local pressures could also be attributable to differences among the model buildings, like lower roof slope, location of pressure taps, and wind flow characteristics in the respective tunnels.

- The literature review appears to show that North American design wind load provisions for sawtooth roofs are based on wind tunnel studies by Saathoff and Stathopoulos (1992), while the Australian/New Zealand provisions are based on the comparable studies by Holmes (1983, 1984, 1987). That higher peak pressure coefficients were obtained in the former study as compared with the latter appears to be the reason why current the North American wind design codes specify larger loads for the sawtooth roof buildings than the Australian/New Zealand wind load design standard.
- The area-averaged pressure coefficients exhibit more rapid falloff with increasing tributary areas than was found in the previous studies. Fifty percent or greater reduction in peak coefficients can be expected on the windward span of a sawtooth roof and on a monosloped roof structure for tributary areas as small as 2.5 m^2 at full scale.

References

ASCE. (1987). "Wind tunnel model studies of buildings and structures." *Manuals and reports on engineering practice*, ASCE, New York.

ASCE/SEI. (2006). "Minimum design loads for buildings and other structures." *ASCE 7-05*, ASCE, Reston, Va.

Cui, B. (2007). "Wind effects on monosloped and sawtooth roofs." Ph.D. thesis, Clemson Univ., Clemson, S.C.

Garg, R. K., Lou, J. X., and Kasperski, M. (1997). "Some features of modeling spectral characteristics of flow in boundary layer wind tunnels." *J. Wind. Eng. Ind. Aerodyn.*, 72(1–3), 1–12.

Holmes, J. D. (1982). "Techniques and modelling criteria for the measurement of external and internal pressures." *Int. Workshop on Wind Tunnel Modeling Criteria and Techniques in Civil Engineering Applications*, Cambridge University Press, Cambridge, England, 245–256.

Holmes, J. D. (1983). "Wind loading of saw-tooth roof buildings—I. Point pressures." *Internal Rep. No. 83/17*, CSIRO, Div. of Building Research, Highett, Australia.

Holmes, J. D. (1984). "Wind loading of saw-tooth roof buildings—II. Panel pressures." *Internal Rep. No. 84/1*, CSIRO, Div. of Building Research, Highett, Australia.

Holmes, J. D. (1987). "Wind loading of multi-span buildings." *First National Structural Engineering Conf.*, Institution of Engineers, Australia, Melbourne, Australia.

Irwin, H. P. A. H., Cooper, K. R., and Girard, R. (1979). "Correction of distortion effects caused by tubing systems in measurements of fluctuating pressures." *Journal of Industrial Aerodynamics*, 5(1–2), 93–107.

Lieblein, J. (1974). "Efficient methods of extreme-value methodology." National Bureau of Standards, Washington, D.C.

Richards, P. J., Hoxey, R. P., Connell, B. D., and Lander, D. P. (2007). "Wind-tunnel modelling of the Silsoe Cube." *J. Wind. Eng. Ind. Aerodyn.*, 95(9–11), 1384–1399.

Saathoff, P. J., and Stathopoulos, T. (1992). "Wind loads on buildings with sawtooth roofs." *J. Struct. Eng.*, 118(2), 429–446.

Standards Australia. (2002). "Australian/New Zealand standard: Structural design actions. Part 2: Wind actions." *AS/NZS 1170.2*, Standards Australia International Ltd., Sydney, Australia.

Stathopoulos, T. (1982). "Techniques and modeling criteria for measuring area averaged pressures." *Int. Workshop on Wind Tunnel Modeling Criteria and Techniques in Civil Engineering Applications*, Cambridge University Press, Cambridge, England, 257–274.

Stathopoulos, T., and Mohammadian, A. R. (1985). "Wind loads on low buildings with mono-sloped roofs." *J. Wind. Eng. Ind. Aerodyn.*, 23(1–3), 81–97.

Stathopoulos, T., and Saathoff, P. (1992). "Codification of wind pressure coefficients for sawtooth roofs." *J. Wind. Eng. Ind. Aerodyn.*, 43(1–3), 1727–1738.

Tieleman, H. W. (1982). "Simulation criteria based on meteorological or theoretical considerations." *Int. Workshop on Wind Tunnel Modeling Criteria and Techniques in Civil Engineering Applications*, Cambridge University Press, Cambridge, England, 73–96.

Tieleman, H. W., Akins, R. E., and Sparks, P. R. (1981). "A comparison of wind tunnel and full-scale wind pressure measurements on low-rise structures." *J. Wind. Eng. Ind. Aerodyn.*, 8, 3–19.